Supplementary Material

Contents:

1. Experimental

All chemicals were purchased from commercial sources. Elemental analysis (C, H and N) was performed on a Vario EL cube (Elementar GmbH) elemental analyzer. The FT-IR spectrum of microcrystalline powder was recorded on a Bruker ALPHA spectrometer with the ATR (attenuated total reflectance) module. Powder X-ray diffraction studies were performed on an Aeris (Malvern PANalytical B.V.) X-ray diffractometer.

Synthesis

Solution of anhydrous cobalt (II) iodide (156.4 mg, 0.5 mmol) and 3,5-dimethylpyrazole (96.1 mg, 1.0 mmol) in dry acetonitrile (4 mL) was stirred for 1 hour at room temperature and then rotary evaporated. Crude product was washed once with cold diethyl ether and thoroughly with hexane. Blue-greenish X-ray quality crystals of the complex were grown by diffusion of hexane into the dichloromethane solution. Yield 148 mg (58.6 %).

Anal. Calc. for $C_{10}H_{16}N_4Co_1I_2$: C, 23.78; H, 3.19; N, 11.09. Found: C, 24.09; H, 3.23; N, 11.32%. IR (neat, cm^{-1}): 3334 (s), 1565 (s), 1469 (m), 1401 (m), 1371 (m), 1274 (s), 1177 (s), 1154 (s), 1115 (m), 1045 (vs), 1022 (m), 980 (w), 800 (s), 663 (w), 651 (vs), 557 (vs), 424 (s). The powder XRD measurements showed that the sample is a monophase crystalline material (Fig. S1). It can be seen that the intensities of the diffraction peaks are redistributed due to crystal texture.

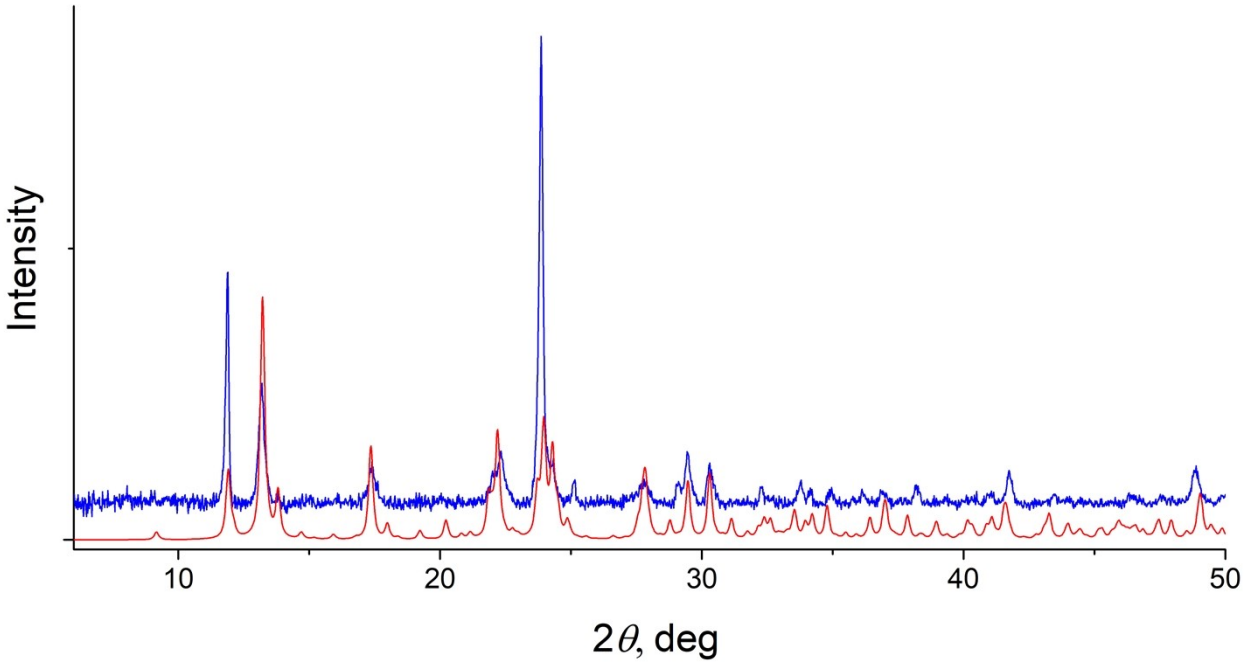

Fig. S1 Powder X-ray diffraction pattern of polycrystalline sample of complex **1**: experimental (top) and simulated (bottom).

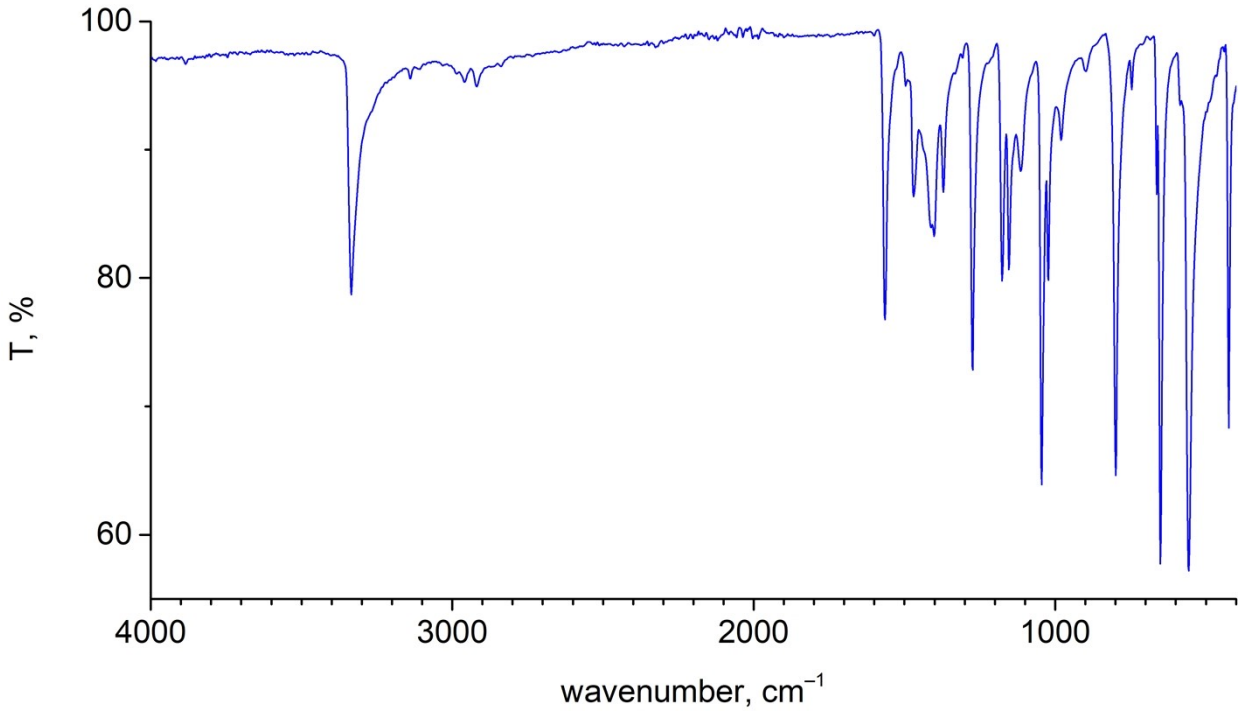

Fig. S2 IR spectrum of polycrystalline sample of complex **1**.

2. X-ray crystallography

X-ray data for a single crystal of **1** (at 100 K) were collected on a CCD diffractometer Agilent XCalibur with EOS detector (Agilent Technologies UK Ltd, Yarnton, Oxfordshire, England) using graphite-monochromated MoK_α radiation (λ = 0.71073 Å). The structure was solved by direct methods and refined against all F^2 data (SHELXTL [1]). All non-hydrogen atoms were refined with anisotropic thermal parameters, positions of hydrogen atoms were obtained from difference Fourier syntheses and refined with riding model constraints. The X-ray crystal structure data have been deposited with the Cambridge Crystallographic Data Center, with reference codes CCDC 2162594. Selected crystallographic parameters and the data collection and refinement statistics are given in Table S2.

Table S1 Crystal data and structure refinement for **1**.

Parameters	**Values**
Temperature, K	100
Empirical formula	$C_{10}H_{16}N_4Co_1I_2$
Molecular weight	505.00
Crystal system, space group	monoclinic, $P2_1/n$
a, Å	8.4778(2)
b, Å	14.8545(3)
c, Å	12.8023(3)
β, °	98.042(2)
Volume, Å^3	1596.39(6)
Z; ρ (calculated), g/cm^3	4; 2.101
μ, mm^{-1}	4.929
F(000)	948
Crystal size, mm^3	0.2 x 0.1 x 0.05
θ range, °	3.043 – 34.069
Reflections collected	25984
Reflections unique [R(int)]	6543 [0.0188]
Completeness to θ = 25.24°	0.999
Number of parameters	158
Goodness-of-fit on F^2	1.071
Final R_1; wR_2 [$I>2\sigma(I)$]	0.0214; 0.0474
R_1; wR_2 (all data)	0.0284; 0.0500
$\Delta\rho_{max}$ and $\Delta\rho_{min}$, e·Å^{-3}	2.350 and -0.501

Table S2 Selected bond lengths (Å) and angles (°) in **1**.

Bond		**Bond**	
Co(1)-I(1)	2.5946(2)	Co(1)-I(2)	2.5742(2)
Co(1)-N(1)	2.001(1)	Co(1)-N(3)	2.008(1)
N(2)-N(1)	1.3613(18)	N(4)-N(3)	1.3603(18)
N(1)-C(4)	1.345(2)	C(7)-N(3)	1.341(2)
N(2)-C(2)	1.348(2)	N(4)-C(9)	1.347(2)
C(1)-C(2)	1.486(2)	C(7)-C(6)	1.492(2)
C(2)-C(3)	1.378(2)	C(9)-C(8)	1.380(2)
C(4)-C(3)	1.396(2)	C(7)-C(8)	1.397(2)
C(4)-C(5)	1.494(2)	C(10)-C(9)	1.493(2)
Angle		**Angle**	
I(2)-Co(1)-I(1)	114.497(9)	N(1)-Co(1)-N(3)	107.39(6)
N(1)-Co(1)-I(2)	115.45(4)	N(3)-Co(1)-I(1)	115.48(4)
N(1)-Co(1)-I(1)	101.57(4)	N(3)-Co(1)-I(2)	102.75(4)
C(2)-N(2)-N(1)	112.09(13)	C(9)-N(4)-N(3)	111.91(13)
C(4)-N(1)-N(2)	105.39(13)	C(7)-N(3)-N(4)	105.57(13)
C(4)-N(1)-Co(1)	131.45(11)	C(7)-N(3)-Co(1)	130.94(11)
N(2)-N(1)-Co(1)	123.15(10)	N(4)-N(3)-Co(1)	123.48(10)
N(2)-C(2)-C(3)	106.04(14)	N(4)-C(9)-C(8)	106.25(14)
N(2)-C(2)-C(1)	122.06(15)	N(4)-C(9)-C(10)	122.16(16)
C(3)-C(2)-C(1)	131.90(16)	C(8)-C(9)-C(10)	131.59(16)
N(1)-C(4)-C(3)	109.76(14)	N(3)-C(7)-C(8)	109.88(15)
N(1)-C(4)-C(5)	120.52(15)	N(3)-C(7)-C(6)	120.29(15)
C(3)-C(4)-C(5)	129.72(15)	C(8)-C(7)-C(6)	129.82(16)
C(2)-C(3)-C(4)	106.71(15)	C(9)-C(8)-C(7)	106.38(15)

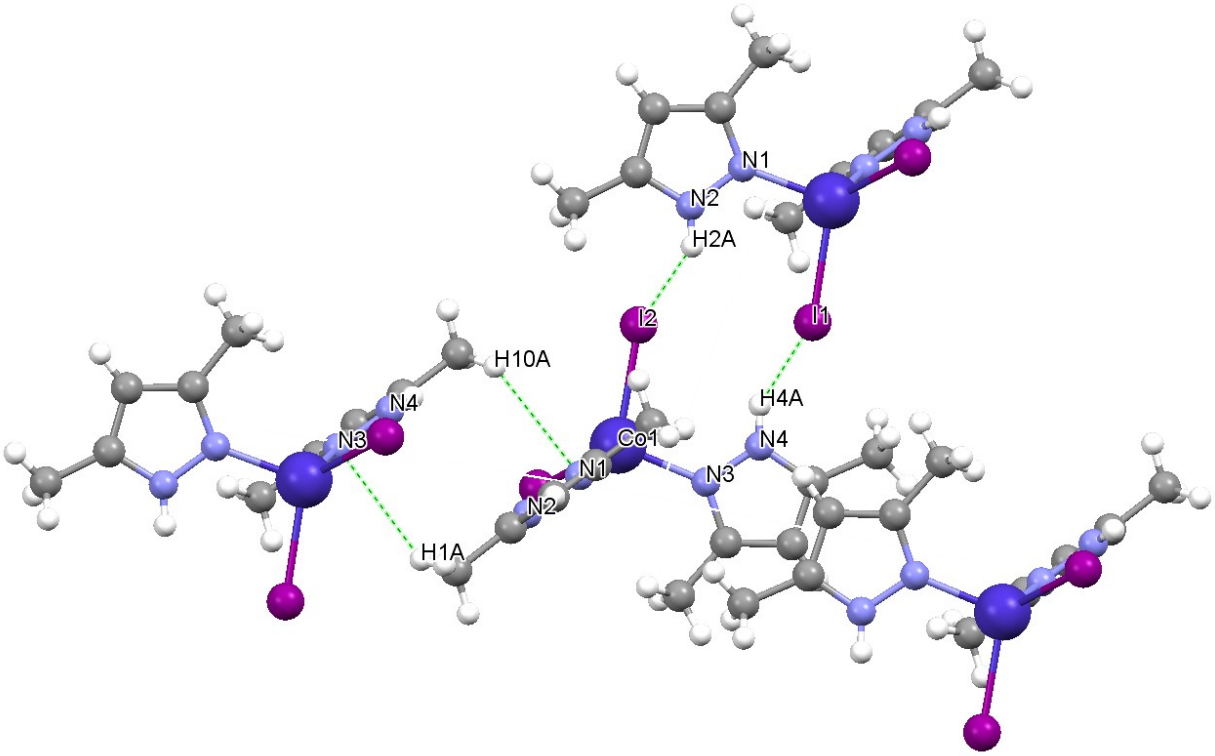

Fig. S3 View of the intermolecular interactions (N–H…I) and (C–H…π) in the crystal structure of **1**. The dashed lines represent shortest distances. N(3)…H(1A) = 2.944 Å, N(1)…H(10A) = 2.904 Å.

Table S3 The local symmetry of Co(II) ion in **1** defined by the continuous shape measure (CShM) analysis with *SHAPE* software.

	Square planar (D_{4h})	Tetrahedron (T_d)	Seesaw (C_{2v})	Vacant trigonal bipyramid (C_{3v})
CShM	29.307	1.959	8.018	3.552

3. Computational details

Theoretical calculations of the electronic structure for complex **1** were performed using a post-Hartree-Fock multi-reference wavefunction (WF) approach based on state-averaged complete active space self-consistent field calculations (SA-CASSCF) [2–4] followed by N-electron valence second-order perturbation theory (NEVPT2) [5–8]. Scalar relativistic effects were accounted for by using a standard second-order Douglas-Kroll-Hess (DKH) procedure [9]. For calculations, a segmented all-electron relativistically contracted version [10] of Ahlrichs polarized triple-zeta basis set, def2-TZVP [11–13], was used for all atoms. To improve the

calculation time, the resolution of the identity approximation with corresponding correlation fitting of the basis set [14] was employed. Spin-orbit effects were included using the quasi-degenerate perturbation theory (QDPT) [15].

The CASSCF active space was constructed from 5 MOs with predominant contributions of 3d-AOs from the metal center and 7 electrons, corresponding to metal ion CAS(7, 5). Ten quartets and 40 doublet states were included in the WF expansion.

4. Magnetic measurements

The magnetic behavior was studied using the Quantum Design PPMS-9 physical property measuring system with the option of measuring dynamic (ac) and static (dc) magnetic susceptibility. This equipment allows research to be carried out in the temperature range of 2–300 K with magnetic fields up to 9 T. During ac susceptibility measurements, an alternating magnetic field amplitude was H_{ac}= 1–5 Oe in the frequency range 10 000–10Hz. The measurements were carried out on polycrystalline samples moistened with mineral oil to prevent the orientation of the crystals in dc magnetic field. The prepared samples were sealed in plastic bags. The magnetic susceptibility χ was determined taking into account the diamagnetic contribution of the substance, using the Pascal scheme, the contribution of the bag and that of mineral oil. PHI program [16] was used for fitting DC magnetic data. The frequency dependences of the ac susceptibility measured at different temperatures were fitted with generalized and two-component Debye model for zero dc and applied H_{dc} = 1500 Oe field, respectively (Table S4 and S5). CC-FIT program [17] was used for fitting AC data.

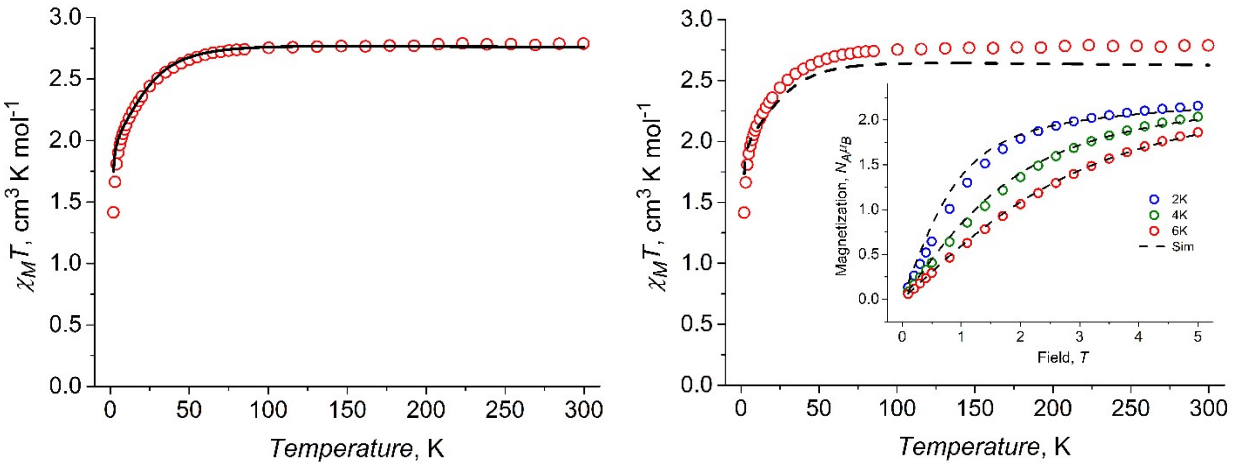

(a) (b)

Fig. S4 Temperature dependences of $\chi_M T$ for **1** measured at H = 0.5 T (open circles). Inset(b): Magnetization vs. field for **1** measured at T = 2, 4 and 6 K (open circles). Solid and dashed lines show the simulated curves without zJ (other best-fit SH parameters listed in text) and within SA-CASSCF/NEVPT2 calculated SH parameters, respectively.

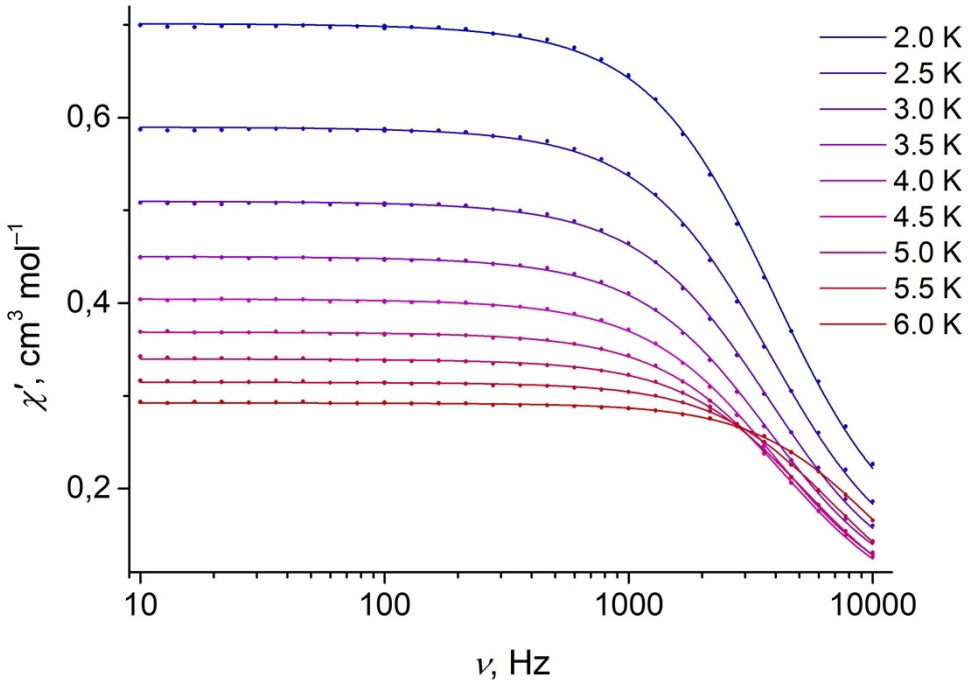

(a)

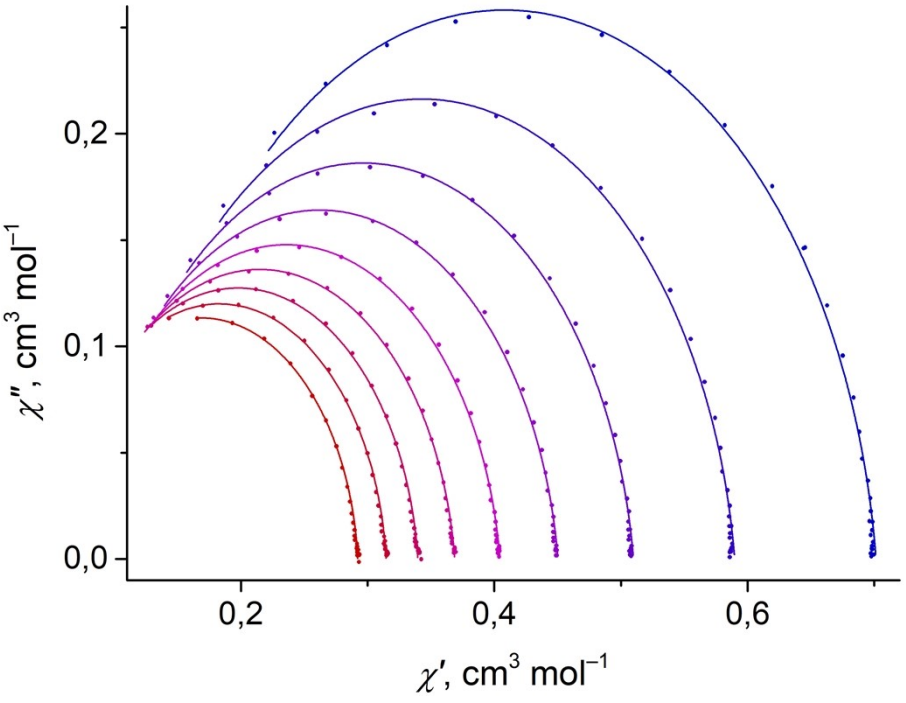

(b)

Fig. S5 (a) Frequency dependence of in-phase (χ_M') susceptibility for complex **1** at the temperature range 2–6 K at zero dc field. (b) Cole-Cole plots. Solid lines represent the best fit.

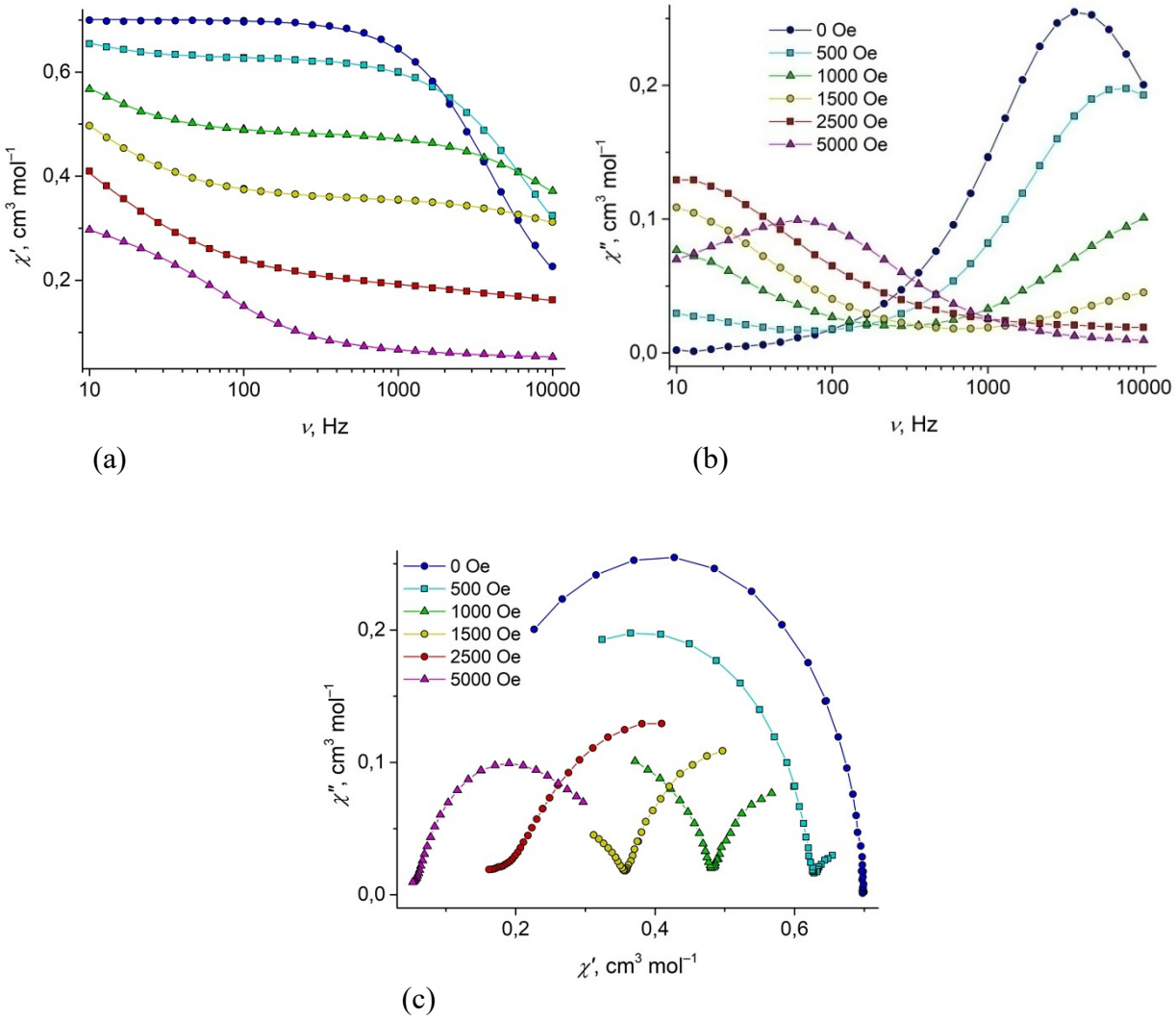

Fig. S6 Frequency dependence of (a) in-phase (χ_M') and (b) out-of-phase (χ_M'') susceptibilities for complex **1** at the temperature 2 K and the dc field range 0–5000 Oe. (c) Cole-Cole plots.

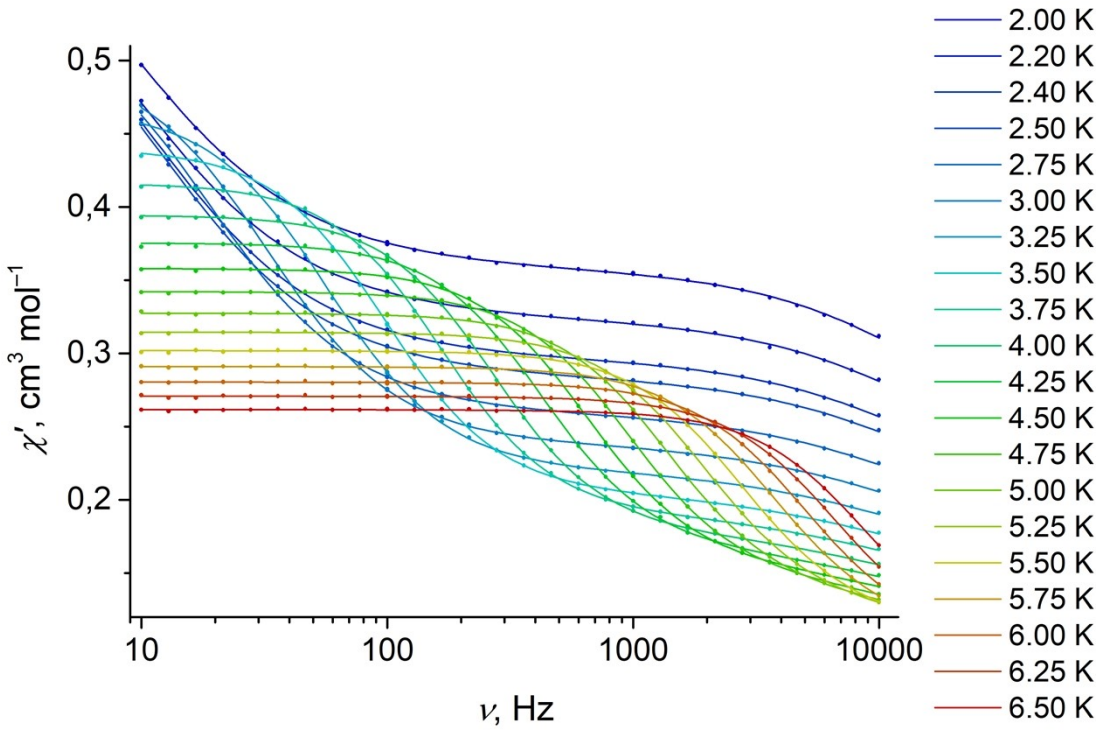

(a)

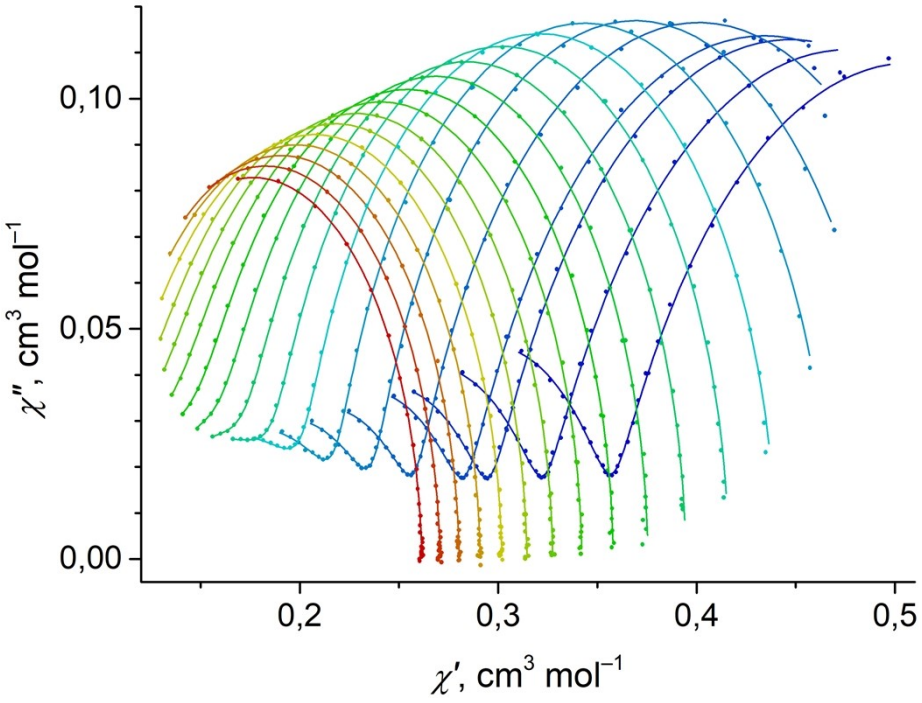

(b)

Fig. S7 (a) Frequency dependence of in-phase (χ_M') susceptibility for complex **1** at the temperature range 2–6.5 K and dc field 1500 Oe. (b) Cole-Cole plots. Solid lines represent the best fit.

Table S4 Best fit parameters of the generalized Debye model for complex **1** at zero dc field.

T, K	χ_S, cm^3 mol^{-1}	$\Delta\chi_T$, cm^3 mol^{-1}	τ, s	α
2.0	0.115	0.587	4.03E-05	0.081
2.5	0.095	0.494	4.15E-05	0.085
3.0	0.084	0.426	4.25E-05	0.086
3.5	0.074	0.376	4.24E-05	0.086
4.0	0.067	0.337	4.06E-05	0.083
4.5	0.061	0.308	3.65E-05	0.077
5.0	0.056	0.284	3.02E-05	0.068
5.5	0.051	0.263	2.31E-05	0.059
6.0	0.046	0.247	1.63E-05	0.054

Table S5 Best fit parameters of the two-component Debye model for complex **1** at 1500 Oe dc field.

T, K	χ_S, cm^3 mol^{-1}	$\Delta\chi_{T1}$, cm^3 mol^{-1}	τ_1, s	α_1	$\Delta\chi_{T2}$, cm^3 mol^{-1}	τ_2, s	α_2
2.0	0.233	0.304	1.80E-02	0.216	0.124	1.06E-05	0.191
2.2	0.209	0.308	1.69E-02	0.208	0.114	1.02E-05	0.205
2.4	0.194	0.305	1.43E-02	0.190	0.101	1.08E-05	0.202
2.5	0.183	0.303	1.29E-02	0.181	0.100	1.02E-05	0.210
2.75	0.166	0.286	8.43E-03	0.133	0.092	1.03E-05	0.231
3.0	0.149	0.262	4.86E-03	0.077	0.090	9.89E-06	0.261
3.25	0.138	0.247	2.79E-03	0.045	0.084	9.69E-06	0.277
3.5	0.128	0.233	1.63E-03	0.025	0.079	9.83E-06	0.290
3.75	0.120	0.223	9.65E-04	0.014	0.074	9.77E-06	0.290
4.0	0.113	0.213	5.94E-04	0.009	0.069	9.82E-06	0.290
4.25	0.106	0.204	3.77E-04	0.006	0.066	9.52E-06	0.291
4.5	0.098	0.196	2.48E-04	0.005	0.064	8.60E-06	0.290
4.75	0.092	0.188	1.67E-04	0.003	0.062	7.80E-06	0.289
5.0	0.083	0.182	1.16E-04	0.003	0.063	5.98E-06	0.289
5.25	0.077	0.177	8.19E-05	0.003	0.061	4.83E-06	0.289
5.5	0.071	0.171	5.92E-05	0.002	0.059	3.95E-06	0.284
5.75	0.067	0.165	4.37E-05	0.002	0.059	3.47E-06	0.285
6.0	0.060	0.162	3.25E-05	0.002	0.058	2.16E-06	0.287
6.25	0.057	0.156	2.45E-05	0.002	0.058	2.01E-06	0.288
6.5	0.053	0.151	1.86E-05	0.003	0.057	1.60E-06	0.287

5. References

1. G. M. Sheldrick (8/06/2000). SHELXTL v. 6.14, Structure Determination Software Suite, Bruker AXS, Madison, Wisconsin, USA.
2. B. O. Roos, P. R. Taylor and P. E. M. Sigbahn, *Chem. Phys.*, 1980, **48**, 157–173.
3. S. Per, H. Anders, R. Björn and L. Bernard, *Phys. Scr.*, 1980, **21**, 323.
4. P. E. M. Siegbahn, J. Almlöf, A. Heiberg and B. O. Roos, *J. Chem. Phys.*, 1981, **74**, 2384–2396.
5. C. Angeli, R. Cimiraglia, S. Evangelisti, T. Leininger and J. P. Malrieu, *J. Chem. Phys.*, 2001, **114**, 10252–10264.
6. C. Angeli, R. Cimiraglia and J.-P. Malrieu, *Chem. Phys. Lett.*, 2001, **350**, 297–305.
7. C. Angeli and R. Cimiraglia, *Theor. Chem. Acc.*, 2002, **107**, 313–317.
8. C. Angeli, R. Cimiraglia and J.-P. Malrieu, *J. Chem. Phys.*, 2002, **117**, 9138–9153.
9. B. A. Hess, *Phys. Rev. A*, 1986, **33**, 3742–3748.
10. D. A. Pantazis, X. Y. Chen, C. R. Landis and F. Neese, *J. Chem. Theory Comput.*, 2008, **4**, 908.
11. A. Schafer, C. Huber and R. Ahlrichs, *J. Chem. Phys.*, 1994, **100**, 5829–5835.
12. A. Schafer, H. Horn and R. Ahlrichs, *J. Chem. Phys.*, 1992, **97**, 2571–2577.
13. F. Weigend and R. Ahlrichs, *PCCP*, 2005, **7**, 3297–3305.
14. F. Neese, *J. Comput. Chem.*, 2003, **24**, 1740–1747.
15. D. Ganyushin and F. Neese, *J. Chem. Phys.*, 2006, **125**, 024103.
16. N. F. Chilton, R. P. Anderson, L. D. Turner, A. Soncini and K. S. Murray, *J. Comput. Chem.*, 2013, **34**, 1164–1175.
17. N. F. Chilton, CC-Fit, The University of Manchester, UK, 2014.